

UCSF

UC San Francisco Previously Published Works

Title

Chewing-Activated TRPV4/PIEZO1-HIF-1 α -Zn Axes in a Rat Periodontal Complex.

Permalink

<https://escholarship.org/uc/item/3zx3f89r>

Journal

Journal of Dental Research, 104(4)

Authors

Wang, Yongmei

Lee, B

Yang, Z

et al.

Publication Date

2025-04-01

DOI

10.1177/00220345241294001

Peer reviewed

Chewing-Activated TRPV4/PIEZO1-HIF-1 α -Zn Axes in a Rat Periodontal Complex

Journal of Dental Research
2025, Vol. 104(4) 398–407
© The Author(s) 2025



Article reuse guidelines:
sagepub.com/journals-permissions
DOI: 10.1177/00220345241294001
journals.sagepub.com/home/jdr

Y. Wang¹ , B.H. Lee¹ , Z. Yang¹, T.J. Ho¹, H. Ci^{2,3,4,5} , B. Jackson⁶, T. Pushon⁶, B. Wang^{2,3,4,5}, J. Levy⁷, and S.P. Ho^{1,8}

Abstract

The upstream mechanobiological pathways that regulate the downstream mineralization rates in periodontal tissues are limitedly understood. Herein, we spatially colocalized and correlated compression and tension strain profiles with the expressions of mechanosensory ion channels (MS-ion) TRPV4 and PIEZO1, biometal zinc, mitochondrial function marker (*MFN2*), cell senescence indicator (*p16*), and oxygen status marker hypoxia-inducible factor-1 α (*HIF-1 α*) in rats fed hard and soft foods. The observed zinc and related cellular homeostasis in vivo were ascertained by TRPV4 and PIEZO1 agonists and antagonists on human periodontal ligament fibroblasts ex vivo. Four-week-old male Sprague-Dawley rats were fed hard ($n = 3$) or soft ($n = 3$) foods for 4 wk (in vivo). Significant changes in alveolar socket and root shapes with decreased periodontal ligament space and increased cementum volume fraction were observed in maxillae on reduced loads (soft food). Reduced loads impaired distally localized compression-stimulated PIEZO1 and mesially localized tension-stimulated TRPV4, decreased mitochondrial function (*MFN2*), and increased cell senescence in mesial and distal periodontal regions. The switch in *HIF-1 α* from hard food–distal to soft food–mesial indicated a plausible effect of shear-regulated blood and oxygen flows in the periodontal complex. Blunting or activating TRPV4 or PIEZO1 MS-ion channels by channel-specific antagonists or agonists in human periodontal ligament fibroblast cultures (in vitro) indicated a positive correlation between zinc levels and zinc transporters but not with MS-ion channel expressions. The effects of reduced chewing loads in vivo were analogous to TRPV4 and PIEZO1 antagonists in vitro. Study results collectively illustrated that tension-induced TRPV4 and compression-induced PIEZO1 activations are necessary for cell metabolism. An increased hypoxic state with reduced functional loads can be a conducive environment for cementum growth. From a practical standpoint, dose rate–controlled loads can modulate tension and compression-specific MS-ion channel activation, cellular zinc, and *HIF-1 α* transcription. These mechanobiochemical events indicate the plausible catalytic role of biometal zinc in mineralization, periodontal maintenance, and dentoalveolar joint function.

Keywords: mastication, zinc, mitochondria, biomechanics, reactive oxygen species, ion channels

Introduction

Sustained mechanical loads (chewing and therapeutic) on the periodontal complex affect the turnover rate of the innervated and vascularized periodontal ligament (PDL), and volume fractions and mineral densities of alveolar bone and cementum, and the PDL-space. These physicochemical changes significantly influence the overall shapes of the alveolar socket and root (Niver et al. 2011). Significant changes in shapes (forms) affect mechanically coupled fluid flow and overall biomechanics of the dentoalveolar joint. From a multiscale biomechanics point of view, the effects of these physicochemical changes are consistently observed as shifts in physical deformations and shear flow of blood and interstitial fluids within the periodontal complex (Jang et al. 2021). A plethora of literature illustrates uniform rates of mesial mineral formation and distal resorption in the periodontal complex of rodents (Sicher and Weinmann 1944; Wang, Ustrian, et al. 2022). However, it is important to note that the biomechanically activated upstream signaling pathways that regulate downstream biological events, resulting in mineral formation and resorption in the periodontal complex, are not well understood.

Joint biomechanics triggers ultrarapid mechanotransduction through tissue-specific mechanosensory ion (MS-ion) channels

¹Department of Preventive and Restorative Dental Sciences, School of Dentistry, University of California, San Francisco, CA, USA

²State Key Laboratory of Structural Analysis for Industrial Equipment, Department of Engineering Mechanics, Dalian University of Technology, Dalian, China

³International Research Center for Computational Mechanics, Dalian University of Technology, Dalian, China

⁴Ningbo Institute of Dalian University of Technology, Ningbo, China

⁵DUT-BSU Joint Institute, Dalian University of Technology, Dalian, China

⁶Department of Biological Sciences, Dartmouth College, Hanover, NH, USA

⁷Department of Pathology and Computational Biomedicine, Cedars Sinai, Los Angeles, CA, USA

⁸Department of Urology, School of Medicine, University of California, San Francisco, CA, USA

A supplemental appendix to this article is available online.

Corresponding Author:

S.P. Ho, University of California, 513 Parnassus Ave, HSW 813, San Francisco, CA 94143, USA.
Email: sunita.ho@ucsf.edu

(Botello-Smith et al. 2019; Cox et al. 2019). Two such MS-ion channels, PIEZO1 and transient receptor potential vanilloid 4 (TRPV4), were identified in the dentoalveolar joint (O’Conor et al. 2014; Zhang et al. 2022). MS-ion channels sensitive to divalent cations calcium (Ca²⁺), magnesium (Mg²⁺), and zinc (Zn²⁺) have been shown to control downstream effector molecules that affect nucleation and dissolution of minerals in bones (Mayer et al. 1994; Kara et al. 2009; Sun et al. 2019; Wang, You, et al. 2022), cartilage (O’Conor et al. 2014), tendons (Ji and McCulloch 2021), and the PDL (Jiang et al. 2021). As compared with the advanced research on Ca²⁺ and Mg²⁺ metabolism and their presence in mineralized tissues, if or how Zn²⁺ concentrations fluctuate in response to chewing magnitude and frequency and sequential downstream intracellular events in the periodontal complex are not known. In particular, the conversion of magnitude and frequency of chewing loads on the dentoalveolar joint into intracellular tissue-specific biochemical signals and anatomy-specific mineralization in a periodontal complex remains unknown.

Materials and Methods

For detailed materials and methods, see Appendix.

In Vivo: Specimens from Preclinical Animal Models

The chewing regimen of Sprague-Dawley male rats (Charles River Laboratories) was regulated as stated previously (Niver et al. 2011). Six 3-wk-old male rats (developing) were fed hard food (HF) pellets (PicoLab Rodent Diet 20 5053; LabDiet) for 1 wk and then randomly separated into 2 groups to be given either HF ($n = 3$) or soft food (SF; $n = 3$) for an additional 4 wk (Niver et al. 2011) (Fig. 1A). Rats were euthanized at 8 wk per the ARRIVE guidelines (Animal Research: Reporting of In Vivo Experiments; Institutional Animal Care and Use Committee protocol AN183106-03, University of California San Francisco).

Dentoalveolar Joint Biomechanics, Stiffness, Bone Strain, and Permeability. Intact left maxillae were dissected for functional imaging (Wang et al. 2020) and processed for histology. Specimens (4 hemimaxilla: 2 each from HF and SF) were loaded to 15 N, and joint stiffness (Newton per millimeter) was estimated from the force-displacement curve (Lin et al. 2014) (Appendix Fig. 1). Digital computed tomography volumes at no load and under load were used to estimate anatomy-specific strains in the bone (Wang et al. 2020). Permeability in meters squared was computed with Porous Microstructure Analysis version 3.1.7.

Spatial Localization of Biomolecules in the Periodontal Complex. The 8- μ m sections from fixed (10% neutral buffered formalin) and decalcified (20% EDTA) right maxillae were immunolocalized with the antibodies against TRPV4, PIEZO1, mitofusin 2, hypoxia-inducible factor 1 α (HIF-1 α), and *p16*. Some sections were further reacted with FluoZin3 and colocalized with PIEZO1 or TRPV4. Sections were counterstained

with hematoxylin (immunohistochemistry) or DAPI (immunofluorescence). Three sections per animal per group were imaged by a light microscope (AXIO-Z3; Zeiss), and quantitative spatial maps of immunolocalized biomolecules (immunohistochemistry and immunofluorescence) were generated with ImageJ (Schneider et al. 2012).

Spatial Localization of Elements in the Periodontal Complex. Spatial elemental concentrations were collected from thin sections of rat maxillae with laser ablation inductively coupled plasma time-of-flight mass spectrometry. The laser spot was 6 μ m with a 30- μ m overlap; the single-pulse response was 5 milliseconds. Results were presented as parts per million. Box plots were generated, and an unpaired Student’s *t* test with $P < 0.05$ was used to identify differences across groups.

In Vitro: Agonist and Antagonist Treatments of MS-Ion Channels to Visualize and Quantify Intracellular Zn and Related Biomolecules in Human PDL Fibroblasts

Human PDL fibroblasts (Lonza Bioscience) were treated with agonists to activate, or antagonists to disable, PIEZO1 and TRPV4 (Appendix Table 1) at day 3 (D3; early stage), day 7 (D7; middle stage), and day 14 (D14; late stage). The concentrations (for dose, see Appendix Table 2) were selected according to MTT assay (Appendix Fig. 3A). Zn in cells was detected by treating them with FluoZin3 for 2 h. Following fixation with 4% paraformaldehyde/phosphate-buffered saline and counterstain with DAPI, cells were imaged with a light microscope. Total RNA was extracted from human PDL fibroblast cultures treated by vehicle or PIEZO1/TRPV4 agonists and antagonists with the RNeasy Mini Kit (Qiagen). Gene expressions of *PIEZO1*, *TRPV4*, *ZIP8*, *ZnT1*, *MFN2*, *HIF-1 α* , and *SOD2* were determined by real-time quantitative PCR (qPCR; for primers, see Appendix Table 2).

Statistical Analyses for Models In Vivo and In Vitro

An unpaired Student’s *t* test with $P < 0.05$ was used to identify anatomy-specific statistical significance in 1) mechanical strains in bone and permeability and 2) differential expression and abundance between all parameters and markers (metals, biomolecules) in HF and SF groups in vivo, and agonist and antagonist groups in vitro.

Immunolocalized Biomolecules In Vivo. Three animals from each group in vivo and 3 wells from each group in vitro were used to identify differences between the HF and SF groups and between the agonist and antagonist groups. Results from cell culture models in vitro and qPCR are expressed as a percentage of vehicle-treated controls. Results from histology sections taken from preclinical animal models are presented as mean \pm SD for each group. Significant differences ($P < 0.05$) between groups were identified as stated previously.

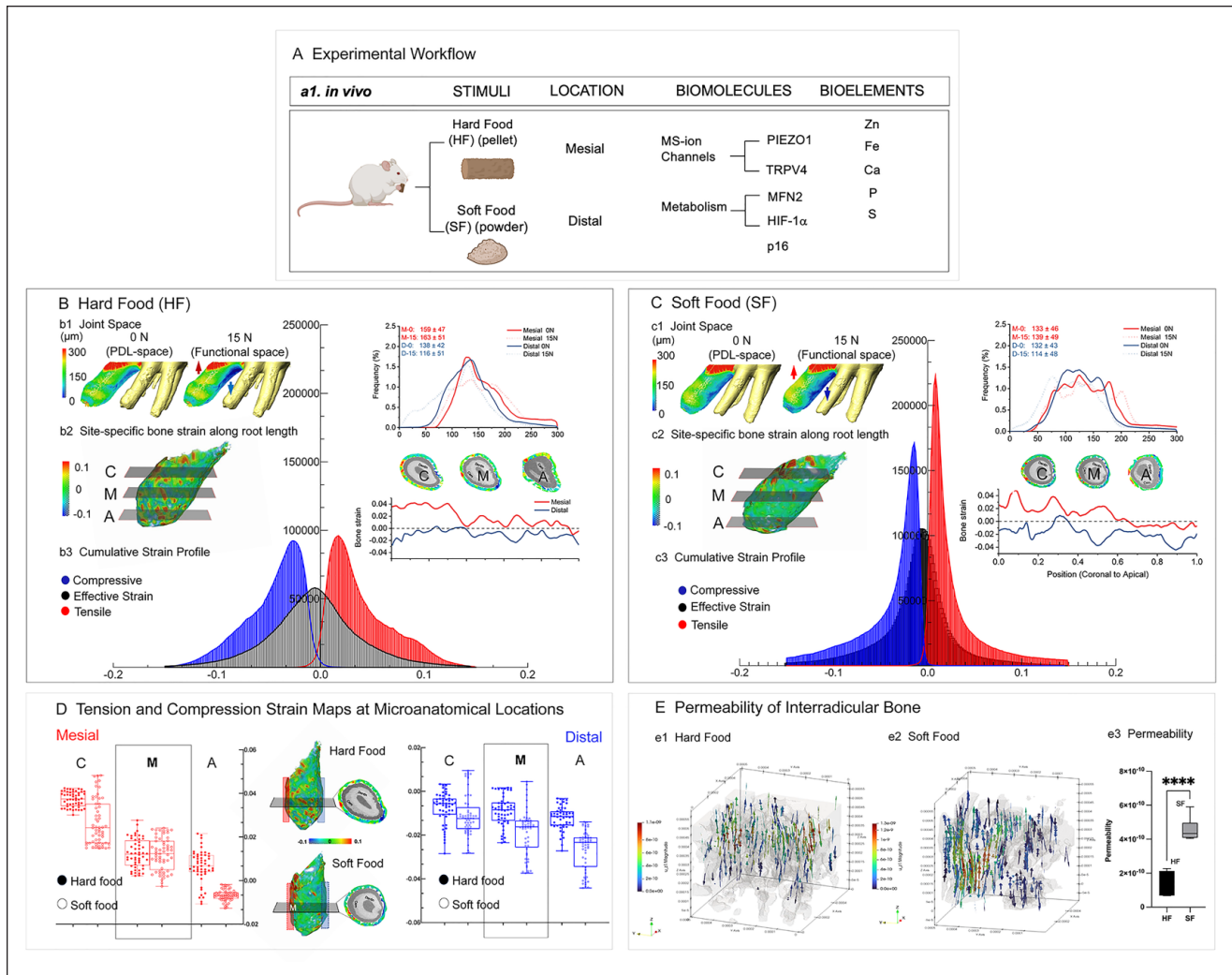


Figure 1. Physical properties of rat maxillary alveolar bones from hard and soft food groups. **(A)** Experimental workflow in which rats were given hard food (HF) or soft food (SF) and mesial and distal anatomical locations were analyzed by multiple analytic techniques and biochemical assays. **(B, C)** Three-dimensional maps of PDL-space at no load (0 N) and under load (15 N) in HF (b1) and SF (c1). Histograms of PDL-space illustrate narrower ranges in HF and SF. Effective strains in bone from coronal to apical regions are shown in a 3-dimensional profile (b2, c2). Line profiles of bone strain along root length suggest distal compression from coronal to apical locations in bone from HF and SF groups. Mesial tension was observed from coronal to apical locations in HF and only in coronal and middle locations of SF. Histograms of strain in bone illustrate lower compressive (blue), tensile (red), and effective strains (black) with higher variance in HF (b3), as opposed to higher strain with less variance in SF (c3). **(D)** Average tension (red) and compression (blue) strains in coronal, middle, and apical locations of mesial and distal anatomic sites of the periodontal complex. **(E)** Permeability of interradicular bone in HF (e1) and SF (e2) groups with observed significant difference (e3) is shown. Data are presented as median, IQR, and 95% CI for box plots or mean (SD) otherwise. **** $P < 0.0001$. A, apical; C, coronal; M, middle; MS-ion, mechanosensory ion; PDL, periodontal ligament.

Correlation and Hierarchical Clustering of Outcomes from In Vivo and In Vitro Models. After stratification by HF/SF status for in vivo replicates and agonist/antagonist status for in vitro replicates, biomarkers and metals were clustered, and Spearman correlation matrices were calculated to determine biomolecular and biometal associations. The PIEZO1/TRPV4 agonists and antagonists were separately clustered globally across all in vitro specimens. Hierarchical clustering was performed independently for D3, D7, and D14 for in vitro experiments, to note if the markers clustered by biological pathway.

Results

Alveolar Bones In Vivo: Higher Effective Strain and Lower Variance in SF but Lower Strain and Higher Variance in HF

Tooth displacement under load was significantly lower in rats that chewed SF than HF (Appendix Fig. 1C) (Niver et al. 2011). A bimodal distribution was observed from the distal (132 to 138 μm) and mesial (133 to 159 μm) PDL space in the

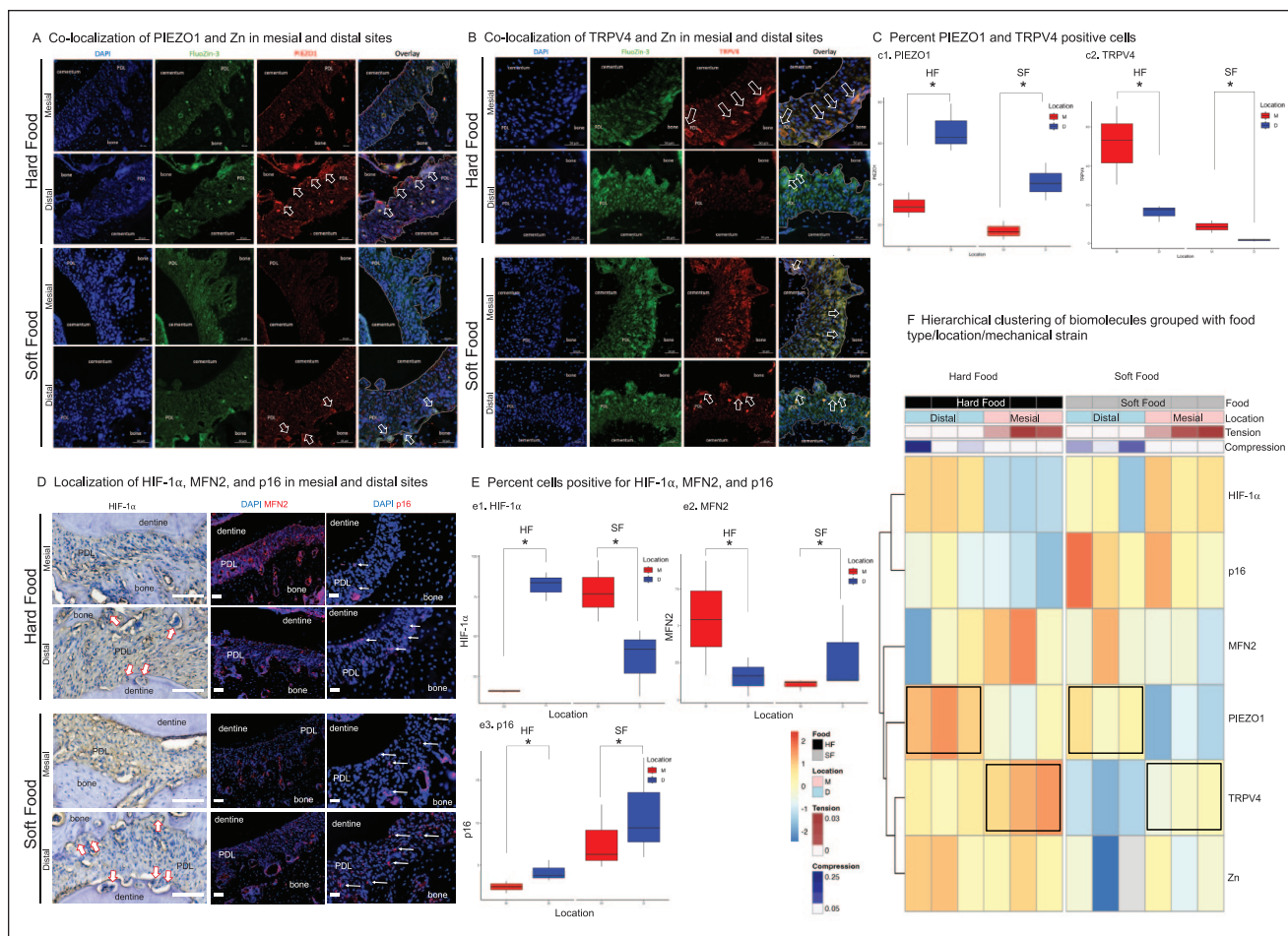


Figure 2. Site-specific mechanosensitive ion localization, mitochondrial function, hypoxia-inducible factor 1 α (HIF-1 α), and cell senescence in the rat periodontal complex can be regulated by food hardness. **(A)** Colocalization of zinc with PIEZO1 illustrated an increased expression in distal versus mesial regions in rats on HF (open arrows). **(B)** Colocalization of zinc with TRPV4 illustrated an increased expression in the mesial side as compared with distal regions in rats on HF (open arrows). **(C)** Significant differences between location-specific (M, D) and food-specific (HF, SF) PIEZO1 and TRPV4 percentage positive cells were observed. **(D)** Biomolecule HIF-1 α , MFN2, and p16 expressions were also location and food hardness specific (white arrows point to resorbed regions in the tooth and bone). **(E)** Significant differences between location- and food-specific HIF-1 α , MFN2, and p16 were observed. **(F)** Hierarchical cluster map illustrated tension-TRPV4-MFN2 axis and compression-PIEZO1-HIF-1 α axis mediated by HF. Location-nonspecific significant increase in cell senescence was observed with SF. Data are presented as median, IQR, and 95% CI for box plots. * $P < 0.05$. D, distal; HF, hard food; M, mesial; PDL, periodontal ligament; SF, soft food.

HF group as compared with the SF group (Fig. 1B-b1, C-c1) (Yang et al. 2019).

Diverse effective strains (combined tensile, compression, and shear strain profiles) were observed within the alveolar bones from both groups (Fig. 1B-b2, C-c2). Bone strain along and across the root suggested mesial tension and distal compression in HF. Higher strains but a uniform profile was observed in the SF group (Fig. 1B-b3, C-c3). The effective strains varied from coronal, mid-, and apical locations in HF (Fig. 1B-b2, D) and SF (Fig. 1C-c2, D). The interradicular bone permeability increased significantly by 3 times in SF as compared with HF (Fig. 1E).

Blunting of TRPV4, PIEZO1, and Zn in SF Rats In Vivo

Experiments in vivo demonstrated biomolecular expression differences by food (HF, SF) and location (anatomically distinct mesial and distal regions). PIEZO1 expression (red, Fig. 2A) in HF was significantly higher ($P < 0.05$) in distal, compressive, and resorptive locations (79% cells) as compared with mesial, tensile, and formative locations (29%). PIEZO1 expressions in SF were impaired in resorptive (32%) and formative (13%) locations (red, Fig. 2A, C-c1). Contrasting PIEZO1, higher TRPV4 expressions were observed at the

formative region (51%) than the resorptive region (16%). TRPV4 expression in formative (9%) and resorptive (2%) locations was impaired in animals that chewed SF (red, Fig. 2B, C-c2). Zn production in the PDL was accompanied by the PIEZO1 expression: higher expression in the distal, compressive, and resorptive region as compared with the mesial, tensile, and formative region in the HF group (green, Fig. 2A). Zn colocalized with PIEZO1 (Fig. 2A) and TRPV4 (Fig. 2B) in PDL cells, and its presence was impaired in the SF group.

In Vivo: Altered Hypoxia, Impaired Mitochondrial Function, and Induced Cell Senescence

Altered Hypoxia. Increased PIEZO1 and HIF-1 α (Fig. 2A, D, E-e1) were observed in distal, compressive, and resorptive cells (82%) than in mesial, tensile, and formative PDL cells (16%) in the HF group. Higher expression of HIF-1 α in mesial (78%) as compared with distal (39%; $P < 0.05$) locations was observed in the SF group (Fig. 2D, E-e1).

Impaired Mitochondrial Function. MFN2 expression in the mesial and formative PDL (82%) was significantly higher than in the distal and resorptive PDL (52%), and this expression pattern was similar to TRPV4 (Fig. 2D). Chewing on softer foods dramatically decreased MFN2 in the mesial (53%) and distal (24%) sides (Fig. 2D, E-e2).

Increased Cell Senescence. Chewing on softer foods increased the number of senescent cells in mesial (8%) and distal (11%) regions (Fig. 2D, E-e3) ($P < 0.05$). In the HF group, p16-positive senescent cells were observed in the distal PDL (5%) as compared with the mesial PDL (3%) (Fig. 2D, E-e3). Significant increases in cell senescence were observed with SF, nonspecific to location.

Food- and Anatomy-Specific Correlation and Clustering of Biomolecular Expressions Suggested MS-Ion Channel Strain-Specific Axes. Spearman correlation matrices indicated relationships between Zn levels and the MS-ion channels, which varied depending on food hardness (Appendix Figs. 2, 4). For HF, Zn levels were negatively associated with TRPV4 expression while positively associated with PIEZO1 expression. For SF, Zn levels were positively associated with TRPV4 expression while negatively associated with PIEZO1 expression. Cluster analysis suggested distinct separation in biomolecular expressions in the periodontal complexes based on food type, with HF and SF diets forming distinct clusters of related biomolecules (Fig. 2F, HF-black, SF-gray). This suggests that the type of diet has a significant impact on the amount of Zn and gene expression (TRPV4, MFN2, PIEZO1, HIF-1 α , and p16). Further stratification within each food group suggested a secondary level of separation corresponding to the anatomic location (Fig. 2F, mesial-pink, distal-blue). Notably, load-induced gene expression gradients were conserved across food types, although there were variations in the degree of expressions, as indicated by box plots (Fig. 2C, E). In clustering the genes,

TRPV4 expression was closely related overall to metabolic programming through its clustering with MFN2, whereas PIEZO1 expression was related to HIF-1 α and p16. Thus, the tension-TRPV4-MFN2 axis and the compression-PIEZO1-HIF-1 α axis are regulated by HF.

Decreased Zn and Iron in the SF PDL In Vivo

Iron (Fe) was detected in the tensile and widened PDL-bone boundary with a rich blood supply (Fig. 3a1, a3) where relatively no HIF-1 α was observed in the HF group in the first root of the first molar (R1M1), according to laser ablation inductively coupled plasma time-of-flight mass spectrometry (Fig. 3). Zn was detected in the compressive and narrow PDL of the R1M1 (Fig. 3a1, a3), as noted by histology (Fig. 2A, B). Fe and Zn concentrations dramatically decreased in the PDL of the R1M1 in the SF group in all locations (Fig. 3a2, a3).

In Vitro: PIEZO1 and TRPV4 Regulate PDL Cell Metabolism and Zn Homeostasis

PIEZO1 Regulates Intracellular Zn and Metabolism in Human PDL Fibroblast Cultures. Intracellular Zn (zincosomes; Appendix Fig. 3A, C-c1, c3) and the RNA levels of ZIP8 and ZnT1 (Appendix Figs. 3C-c2, c4, 4B-b2) increased in the human PDL fibroblast cells from the proliferating (D3 and D7) to fully differentiated (D14) stage with mineralization nodules observed in D14 cultures (Appendix Figs. 3A, 4B). Activation of the PIEZO1 channel by Yoda1 significantly increased intracellular Zn-positive vesicles while blunting the PIEZO1 channel by GsMTx4-decreased intracellular Zn at all stages of the cultures when compared with the vehicle-treated cultures (Fig. 4B-b1, b2). In addition, qPCR indicated that at D14 (Appendix Fig. 3C-c1), the effect of Yoda1 trended and significantly increased intracellular Zn and RNA levels of ZIP8, ZnT1, HIF-1 α , and MFN2 but decreased RNA levels of SOD2 (Fig. 4B-b1, b2).

TRPV4 Channel in Regulating Intracellular Zn Levels and Metabolism in Human PDL Fibroblast Cultures. As shown in Fig. 4 stimulation of the TRPV4 channel by GSK1016790A increased intracellular Zn and RNA levels of ZIP8, ZnT1, HIF-1 α , SOD2, and MFN2, while disabling TRPV4 channel by GSK205 did not significantly affect the intracellular zincosomes, ZIP8 and ZnT1 but increased the RNA levels of HIF-1 α , SOD2, and MFN2 (Fig. 4B-b1, b2). However, the increased levels were not as dramatic as the treatment of the agonist GSK1016790A.

MS-Ion Channel and Zn Transport-Controlled Biomolecular Expressions In Vitro. Similar to our in vivo findings, Spearman correlation matrices—stratified by replicates treated by the agonist and antagonist—suggested positive relationships between Zn levels and Zn transporters but not with MS-ion channel expressions (Appendix Fig. 4A). By D14, hierarchical clustering (Fig. 4b3) suggested clear differences in gene expression profiles. TRPV4 expression showed proximity to metabolic genes such as HIF-1 α and SOD2. Conversely,

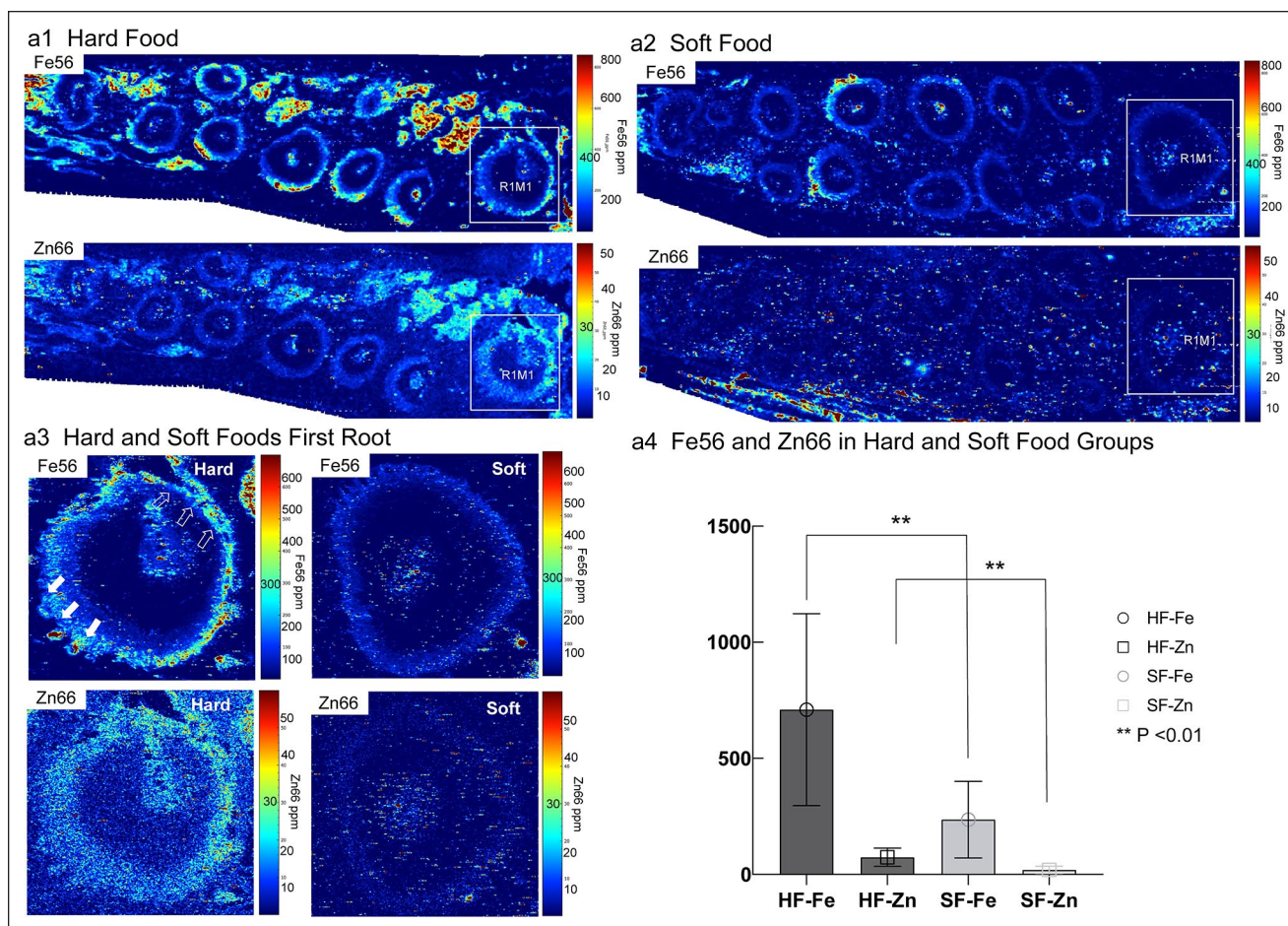


Figure 3. Fe56 and Zn66 concentrations were significantly higher in the HF group as compared with the SF group. Spatial maps of Fe66 (top row) and Zn66 (bottom row) in the hemimaxillae of rats fed HF (a1) or SF (a2). (a3) The first root of the first molar is shown at a higher magnification to illustrate differences in the narrowed (open arrows) and widened (solid arrows) regions of the periodontal complex. (a4) Significant increase in concentrations of Fe66 and Zn66 in hemimaxillae from the HF group as compared with SF group was observed. Data are presented as mean (SD). ** $P < 0.01$. HF, hard food; SF, soft food.

PIEZO1 was clustered near the Zn transporter gene *ZIP8* and the metabolic marker *MFN2*. Upon examination of the data focused solely on agonists and antagonists without the vehicle, the clustering shifted: TRPV4 clustered closer to *ZIP8* (Fig. 4b3). Results on D3-D14 are in Appendix Figure 4B.

Discussion

Followed by Fe, Zn is the second-most abundant trace metal in humans and animals. The importance of extracellular Zn and related bone phenotype (King 1990, 1996; King et al. 2000) at a tissue level is known. MS-ion channels sensitive to divalent cations including Zn^{2+} affect cellular function and nucleation and dissolution of minerals in bones and teeth (Mayer et al. 1994; King 1996; Kara et al. 2009; Sun et al. 2019; Wang, You, et al. 2022). We found that the hard and soft chewing regimens from our model in vivo potentially regulate cellular homeostasis of biometal Zn and its transports (*ZnT1* and *ZIP8*); these results were recapitulated in analogous agonist and antagonist treatments within our cell model in vitro (Figs. 2–4). In

response to mechanical strains, normal intracellular Zn levels are altered to initiate mitochondrial and cytoplasmic signaling events (Fukada et al. 2011) at the microanatomic periodontal locations. The Zn increase at D7 and mineralized nodules at D14 in fibroblast cultures (Appendix Figs. 3A, 4B) suggested the role of Zn in cell maturation and mineralization. Labile intracellular Zn to regulate organelle and cell functions (Bossy-Wetzel et al. 2004; Inoue et al. 2015; Kambe et al. 2015; Deng et al. 2021) and cell fate (Eron et al. 2018) are also known. Intracellular Zn homeostasis is controlled by membrane-bound Zn transporters (*Slc30a* family [Zn transporter]) that export or import (*Slc39a* family [ZIP]) (Cousins et al. 2006) and via storage in organelles (Lu et al. 2016), such as mitochondria and endoplasmic reticulum. Zn transporters tightly control reactive oxygen species (ROS) expression, Zn levels, cellular function, and fate (Maret 2019).

We postulate that the upstream, tension, compression, and shear-induced mechanical strains in vivo can stabilize the HIF-1 α in a tissue- and cell-specific manner and control Zn and ROS (*SOD2*) production by mitochondrial function (*MFN2*)

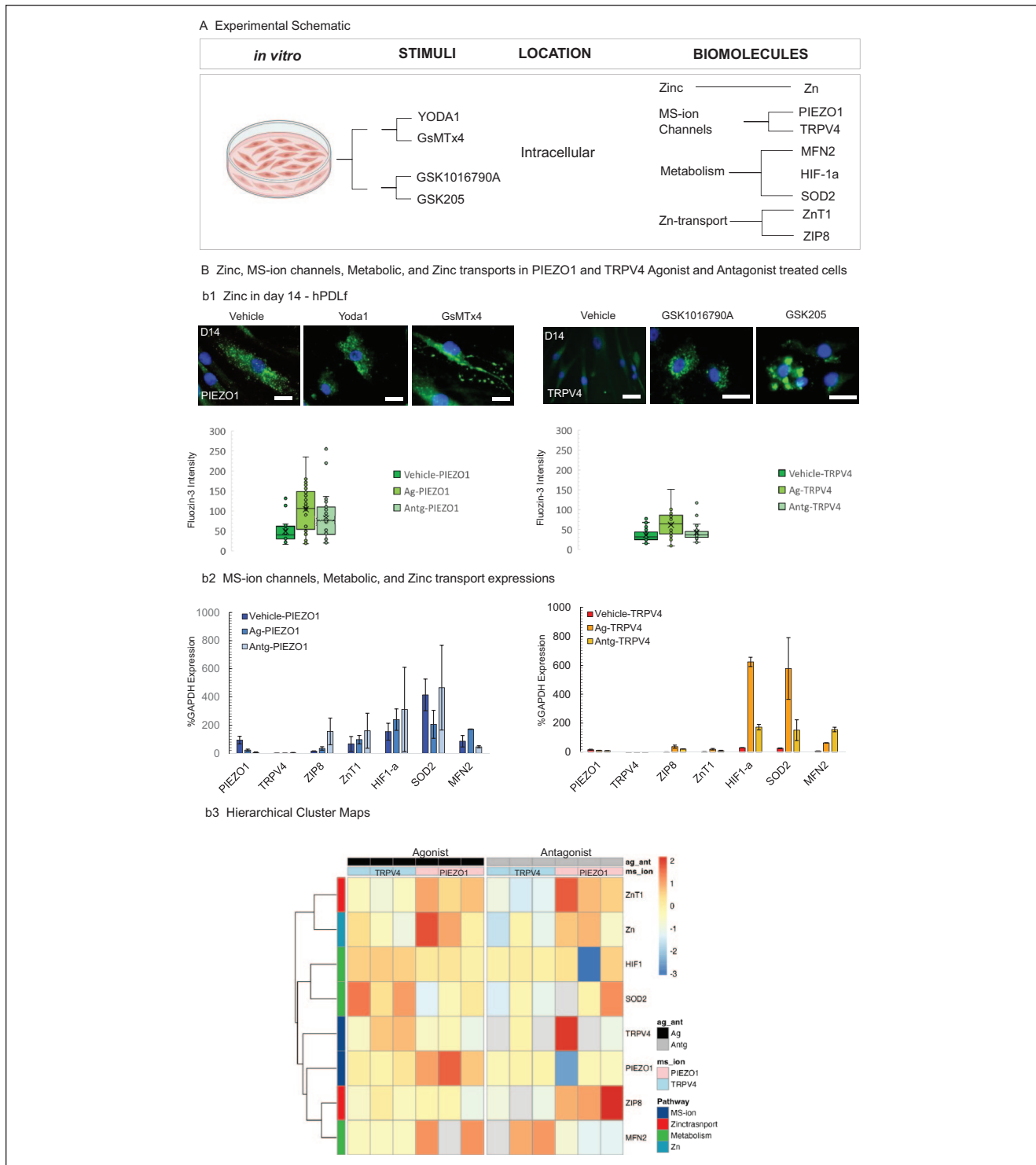


Figure 4. PIEZO1 and TRPV4 regulate intracellular zinc levels and cell metabolism of human PDL fibroblasts *in vitro*. **(A)** Experimental workflow of human PDL fibroblast cultures. **(B)** At day 14, the PIEZO1 channel in human PDL fibroblast cells was activated or disabled by agonist (Yoda1) or antagonist (GsMTx4), respectively. Intracellular zinc was identified by FluoZin3 (b1, green dots) and DAPI-counterstained nuclei. The number of intracellular zinc vesicles (green dots, box plots) are shown. The RNA levels of PIEZO1, TRPV4, ZIP8, ZnT1, HIF-1 α , MFN2, and SOD2 (as measured by quantitative polymerase chain reaction) were calculated and are shown in panel b2, left panel. Similarly, the TRPV4 channel in the human PDL fibroblast cultures was activated or disabled by GSK1016790A or GSK205, respectively (b2, right panel). Scale bars = 20 μ m. (b3) Hierarchical clustering suggested a clear differentiation in that the TRPV4 condition was closely associated with metabolic genes such as HIF-1 α and SOD2. Conversely, PIEZO1 was closely associated with ZIP8 and the metabolic marker MFN2. Upon examination of the data focused solely on agonists and antagonists without the vehicle, the clustering shifted: TRPV4 clustered closer to ZIP8. Results on days 3 through 14 are in Appendix Figure 4. Data are presented as median, IQR, and 95% CI for box plots or mean (SD) otherwise. HIF-1 α , hypoxia-inducible factor-1 α ; MS-ion, mechanosensory ion; PDL, periodontal ligament.

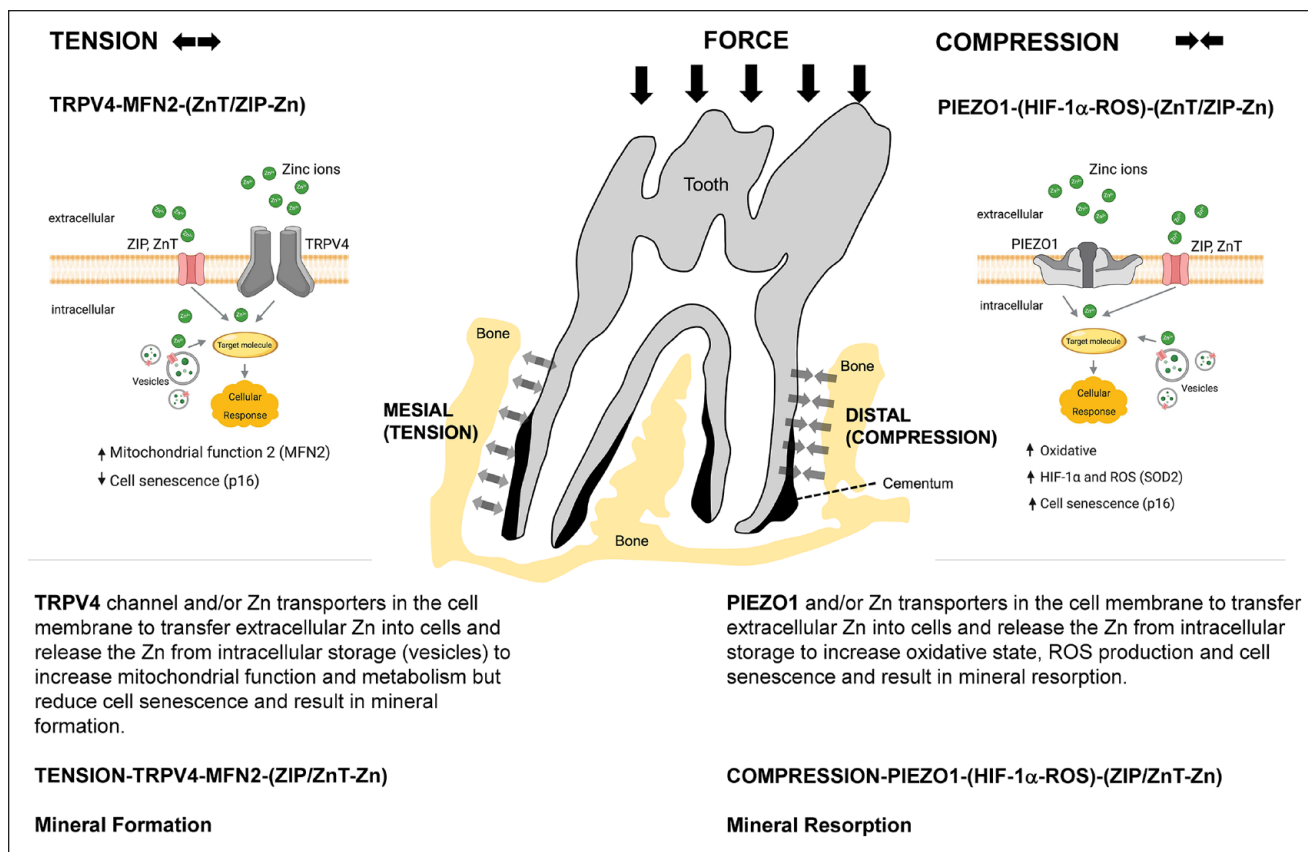


Figure 5. Hypothesized MS-ion channel-regulated biomineralization in the periodontal complex. Mineral formation is regulated by tension-mediated TRPV4 activation (MFN2-ZIP/ZnT-Zn axis) and mineral resorption by compression-mediated PIEZO1 activation (HIF-1 α -ROS-ZIP/ZnT-Zn axis) within the periodontal complex when stimulated by chewing loads. HIF-1 α , hypoxia-inducible factor 1 α ; MS-ion, mechanosensory ion; ROS, reactive oxygen species.

as a potential mediator. The HIF-1 α -induced biochemical cascade can incite downstream oxidative phosphorylation, a necessary step to control tissue-specific cellular function (Sabini et al. 2023). Cellular homeostasis of ROS and resulting oxidative phosphorylation control mineral resorption and formation and maintenance of soft and hard tissue mechanical integrity (Jezek et al. 2010). In our study, compression of blood vessels in the PDL (decreased Fe signal in the narrowed PDL; Fig. 3) → PIEZO1 (Jin et al. 2015) stabilized HIF-1 α (Solis et al. 2019) and decreased mitochondrial fusion (MFN2; Fig. 2) (Xiang et al. 2024), a cascade that resembles ischemia-induced hypoxia, SOD2 production (Xiang et al. 2024) → senescent cells (increased *p16*; Fig. 2) (Ren et al. 2022) but at the distal/compression regions. Mitochondrial function (MFN2) and hypoxia (HIF-1 α) relate to cell senescence (*p16*) (Xing et al. 2018; Miwa et al. 2022). Based on results from this study and literature, we hypothesize that matrix tension → TRPV4 channel → MFN2 but reduced HIF-1 α , and SOD2 (increased Fe signal) in the widened PDL → Zn (Figs. 2, 3). The lower magnitude imparted by SF, however, reduced overall fluid flow, decreasing overall tissue oxygenation (significantly decreased Fe signal in SF group; Fig. 3) and Zn levels, and increased region nonspecific HIF-1 α expression in the periodontal

complex (Fig. 2). Cementum growth was identified (Appendix Fig. 1) (Jang et al. 2015), alluding to the hypothesis stated by others (Choi et al. 2014) that a hypoxic environment encouraged by weak or no occlusal load promotes its growth. Elevated Zn in compressed PDL than in stretched PDL in the HF group contrasted impaired Zn levels in the SF group (Figs. 2, 3), adding to the unexplored role of biometal Zn in microenvironments and its effect on biomineralization in the periodontal complex. These data suggest that HF-induced mechanical strains can regulate intracellular Zn levels and cellular function.

So, how do chewing loads (biomechanical stimuli) and Zn concentrations affect PDL metabolism and cell fate? Our findings, as listed in Figure 5, illustrate that the downstream effects of the mechanical stimuli and Zn homeostasis on PDL cell metabolism and the oxidative state differ by mechanical strain type (stretch, compression, shear) and strain magnitude at the tissue and cell levels. Compression-activated PIEZO1 promotes the influx of extracellular Zn and releases the Zn from the vesicular storage to increase the intracellular labile Zn in a compressed PDL. Higher Zn in compressed PDL cells in a hypoxic environment inhibits mitochondria function (Bossy-Wetzell et al. 2004) and increases ROS production. Contrastingly, our

findings suggest that tensile loads activate TRPV4 to regulate intracellular labile Zn to lower levels, stimulate mitochondria fusion and function, and reduce ROS production in the PDL cells. Thus, in addition to directing MS-ion channel activity, mechanical stimuli potentially maintain metabolism and regulate oxidative stress via the regulation of cellular Zn homeostasis. The mechanoregulation of MS-ion channels and ZnT expressions controlling Zn intracellular and cellular function also can result from 1) activation of PIEZO1 and TRPV4 to import Zn, the levels of which are affected by mechanical loading—coupled tissue oxygenation from the extracellular milieu (Inoue et al. 2015), and 2) mechanically stimulated PIEZO1 and TRPV4, which can affect Zn transporters ZIP8 or ZnT1 (as evidenced through qPCR analysis; Fig. 4) to regulate Zn influx and efflux. Consistent with the *in vivo* findings, PIEZO1 and TRPV4 exhibit opposing expression profiles *in vitro*, highlighting their potentially complementary yet opposing roles in cellular signaling pathways related to mechanical/chemical stimuli. These patterns of gene expressions suggest a complex interplay between mechanical and chemical stimuli in regulating metabolic and mineralization processes.

Observations revealed study limitations (Appendix) and provided plausible insights into the need for solid and fluid mechanics—induced shear flow to maintain Zn-mediated biological pathways in the periodontal complex (Fig. 5). These results corroborated with increased pore volume fraction, reduced alveolar bone mineral density, and increased cementum, which are observed physicochemical changes in a periodontal complex under disuse. In summary (Fig. 5), results suggest that modulation of short- and long-term prescription of a loading regimen (mechanotherapeutics) that constitutes chewing on harder and softer foods can influence MS-ion channels, cellular Zn, and HIF-1 α transcription, as well as the ensuing biomineralization events, periodontal maintenance, and overall dentoalveolar joint function.

Author Contributions

Y. Wang, contributed to conception, design, data acquisition, analysis, and interpretation, drafted and critically revised the manuscript; B.H. Lee, contributed to data acquisition and analysis, worked on figures and tables of the manuscript, cell culture, MTT assays, histology; Z. Yang, contributed to data acquisition and analysis, physical measurements, and computed tomography analysis; T.J. Ho, contributed to data analysis, cell culture studies; H. Ci, contributed to data analysis, strain maps and permeability, and other physical measurements; B. Jackson, T. Pushon, contributed to data acquisition and analysis, worked on laser ablation inductively coupled plasma mass spectrometry; B. Wang, contributed to data acquisition and analysis, worked on mechanical testing and strain mapping; J. Levy, contributed to data analysis and interpretation, bioinformatics/higher-level data analyses; S.P. Ho, contributed to conception, design, data analysis and interpretation, drafted and critically revised the manuscript. All authors gave final approval and agree to be accountable for all aspects of the work.

Acknowledgments

The authors express their sincere thanks for the expert discussions and input from Wolfgang Maret, PhD, Professor of Metallomics, King's College London, on zinc-related redox chemistry and cellular function. The authors thank Putu Ustriyana, Irene Hung, Arman Sheeler, Jasper Chang, Sukhmandeep Sidhu, and Lea Segdhi for their assistance with animal maintenance. The authors thank the Biomaterials and Bioengineering Correlative Microscopy Core, University of California San Francisco, for the use of MicroXCT-200 and biomechanical testing *in situ*. Laser ablation inductively coupled plasma mass spectrometry elemental imaging was performed at the Dartmouth Biomedical National Elemental Imaging Resource, as supported by the National Institute of General Medical Sciences (R24GM141194 and 1S10OD032352).

Funding

The authors disclosed receipt of the following financial support for the research, authorship, and/or publication of this article: This research was supported by the National Institutes of Health/National Institute of Dental and Craniofacial Research (R01 DE022032 to S.P.H.).

ORCID iDs

Y. Wang  <https://orcid.org/0000-0001-6207-9381>

B.H. Lee  <https://orcid.org/0000-0002-2656-6876>

H.Ci  <https://orcid.org/0000-0001-8197-762X>

Data Availability Statement

The data that support the findings of this study are available from the corresponding author upon reasonable request.

References

- Bossy-Wetzel E, Talantova MV, Lee WD, Scholzke MN, Harrop A, Mathews E, Gotz T, Han J, Ellisman MH, Perkins GA, et al. 2004. Crosstalk between nitric oxide and zinc pathways to neuronal cell death involving mitochondrial dysfunction and p38-activated K⁺ channels. *Neuron*. 41(3):351–365.
- Botello-Smith WM, Jiang W, Zhang H, Ozkan AD, Lin YC, Pham CN, Lacroix JJ, Luo Y. 2019. A mechanism for the activation of the mechanosensitive Piezo1 channel by the small molecule Yoda1. *Nat Commun*. 10(1):4503.
- Choi H, Jin H, Kim JY, Lim KT, Choung HW, Park JY, Chung JH, Choung PH. 2014. Hypoxia promotes CEMP1 expression and induces cementoblastic differentiation of human dental stem cells in an HIF-1-dependent manner. *Tissue Eng Part A*. 20(1–2):410–423.
- Cousins RJ, Liuzzi JP, Lichten LA. 2006. Mammalian zinc transport, trafficking, and signals. *J Biol Chem*. 281(34):24085–24089.
- Cox CD, Bavi N, Martinac B. 2019. Biophysical principles of ion-channel-mediated mechanosensory transduction. *Cell Rep*. 29(1):1–12.
- Deng H, Qiao X, Xie T, Fu W, Li H, Zhao Y, Guo M, Feng Y, Chen L, Zhao Y, et al. 2021. SLC-30A9 is required for Zn²⁺ homeostasis, Zn²⁺ mobilization, and mitochondrial health. *Proc Natl Acad Sci U S A*. 118(35):e2023909118.
- Eron SJ, MacPherson DJ, Dagbay KB, Hardy JA. 2018. Multiple mechanisms of zinc-mediated inhibition for the apoptotic caspases-3, -6, -7, and -8. *ACS Chem Biol*. 13(5):1279–1290.
- Fukada T, Yamasaki S, Nishida K, Murakami M, Hirano T. 2011. Zinc homeostasis and signaling in health and diseases: zinc signaling. *J Biol Inorg Chem*. 16(7):1123–1134.
- Inoue K, O'Bryant Z, Xiong ZG. 2015. Zinc-permeable ion channels: effects on intracellular zinc dynamics and potential physiological/pathophysiological significance. *Curr Med Chem*. 22(10):1248–1257.
- Jang A, Wang B, Ustriyana P, Gansky SA, Maslennikov I, Useinov A, Prevost R, Ho SP. 2021. Functional adaptation of interradicular alveolar bone to reduced chewing loads on dentoalveolar joints in rats. *Dent Mater*. 37(3):486–495.

- Jang AT, Merkle AP, Fahey KP, Gansky SA, Ho SP. 2015. Multiscale biomechanical responses of adapted bone–periodontal ligament–tooth fibrous joints. *Bone*. 81:196–207.
- Jezek P, Plecica-Hlavata L, Smolkova K, Rossignol R. 2010. Distinctions and similarities of cell bioenergetics and the role of mitochondria in hypoxia, cancer, and embryonic development. *Int J Biochem Cell Biol*. 42(5):604–622.
- Ji C, McCulloch CA. 2021. TRPV4 integrates matrix mechanosensing with Ca²⁺ signaling to regulate extracellular matrix remodeling. *FEBS J*. 288(20):5867–5887.
- Jiang Y, Guan Y, Lan Y, Chen S, Li T, Zou S, Hu Z, Ye Q. 2021. Mechanosensitive Piezo1 in periodontal ligament cells promotes alveolar bone remodeling during orthodontic tooth movement. *Front Physiol*. 12:767136.
- Jin Y, Li J, Wang Y, Ye R, Feng X, Jing Z, Zhao Z. 2015. Functional role of mechanosensitive ion channel Piezo1 in human periodontal ligament cells. *Angle Orthod*. 85(1):87–94.
- Kambe T, Tsuji T, Hashimoto A, Itsumura N. 2015. The physiological, biochemical, and molecular roles of zinc transporters in zinc homeostasis and metabolism. *Physiol Rev*. 95(3):749–784.
- Kara C, Orbak R, Dagsuyu IM, Orbak Z, Bilici N, Gumustekin K. 2009. In vivo assessment of zinc deficiency on craniofacial growth in a rat model. *Eur J Dent*. 3(1):10–15.
- King JC. 1990. Assessment of zinc status. *J Nutr*. 120 Suppl 11:1474–1479.
- King JC. 1996. Does poor zinc nutrition retard skeletal growth and mineralization in adolescents? *Am J Clin Nutr*. 64(3):375–376.
- King JC, Shames DM, Woodhouse LR. 2000. Zinc homeostasis in humans. *J Nutr*. 130(5S):1360S–1366S.
- Lin JD, Lee J, Ozcoban H, Schneider GA, Ho SP. 2014. Biomechanical adaptation of the bone–periodontal ligament (PDL)–tooth fibrous joint as a consequence of disease. *J Biomech*. 47(9):2102–2114.
- Lu Q, Haragopal H, Slepchenko KG, Stork C, Li YV. 2016. Intracellular zinc distribution in mitochondria, ER and the Golgi apparatus. *Int J Physiol Pathophysiol Pharmacol*. 8(1):35–43.
- Maret W. 2019. The redox biology of redox-inert zinc ions. *Free Radic Biol Med*. 134:311–326.
- Mayer I, Apfelbaum F, Featherstone JD. 1994. Zinc ions in synthetic carbonated hydroxyapatites. *Arch Oral Biol*. 39(1):87–90.
- Miwa S, Kashyap S, Chini E, von Zglinicki T. 2022. Mitochondrial dysfunction in cell senescence and aging. *J Clin Invest*. 132(13):e158447.
- Niver EL, Leong N, Greene J, Curtis D, Ryder MI, Ho SP. 2011. Reduced functional loads alter the physical characteristics of the bone–periodontal ligament–cementum complex. *J Periodontol Res*. 46(6):730–741.
- O’Conor CJ, Leddy HA, Benefield HC, Liedtke WB, Guilak F. 2014. TRPV4-mediated mechanotransduction regulates the metabolic response of chondrocytes to dynamic loading. *Proc Natl Acad Sci U S A*. 111(4):1316–1321.
- Ren X, Li B, Xu C, Zhuang H, Lei T, Jiang F, Zhou P. 2022. High expression of Piezo1 induces senescence in chondrocytes through calcium ions accumulation. *Biochem Biophys Res Commun*. 607:138–145.
- Sabini E, Arboit L, Khan MP, Lanzolla G, Schipani E. 2023. Oxidative phosphorylation in bone cells. *Bone Rep*. 18:101688.
- Schneider CA, Rasband WS, Eliceiri KW. 2012. NIH Image to ImageJ: 25 years of image analysis. *Nat Methods*. 9(7):671–675.
- Sicher H, Weinmann JP. 1944. Bone growth and physiologic tooth movement. *Am J Orthod Oral Surg*. 30(3):C109–C132.
- Solis AG, Bielecki P, Steach HR, Sharma L, Harman CCD, Yun S, de Zoete MR, Warnock JN, To SDF, York AG, et al. 2019. Mechanosensation of cyclical force by PIEZO1 is essential for innate immunity. *Nature*. 573(7772):69–74.
- Sun W, Chi S, Li Y, Ling S, Tan Y, Xu Y, Jiang F, Li J, Liu C, Zhong G, et al. 2019. The mechanosensitive Piezo1 channel is required for bone formation. *Elife*. 8:e47454.
- Wang B, Kim K, Srirangapattanam S, Ustriyana P, Wheelis SE, Fakra S, Kang M, Rodrigues DC, Ho SP. 2020. Mechanoadaptive strain and functional osseointegration of dental implants in rats. *Bone*. 137:115375.
- Wang B, Ustriyana P, Tam CS, Lin JD, Srirangapattanam S, Kapila Y, Ryder MI, Webb S, Seo Y, Ho SP. 2022. Functional adaptation of LPS-affected dentoalveolar fibrous joints in rats. *J Periodontol Res*. 57(1):131–141.
- Wang L, You X, Zhang L, Zhang C, Zou W. 2022. Mechanical regulation of bone remodeling. *Bone Res*. 10(1):16.
- Xiang Z, Zhang P, Jia C, Xu R, Cao D, Xu Z, Lu T, Liu J, Wang X, Qiu C, et al. 2024. Piezo1 channel exaggerates ferroptosis of nucleus pulposus cells by mediating mechanical stress-induced iron influx. *Bone Res*. 12(1):20.
- Xing J, Ying Y, Mao C, Liu Y, Wang T, Zhao Q, Zhang X, Yan F, Zhang H. 2018. Hypoxia induces senescence of bone marrow mesenchymal stem cells via altered gut microbiota. *Nat Commun*. 9(1):2020.
- Yang L, Kang M, He R, Meng B, Pal A, Chen L, Jheon AH, Ho SP. 2019. Microanatomical changes and biomolecular expression at the PDL-entheses during experimental tooth movement. *J Periodontol Res*. 54(3):251–258.
- Zhang M, Meng N, Wang X, Chen W, Zhang Q. 2022. TRPV4 and PIEZO channels mediate the mechanosensing of chondrocytes to the biomechanical microenvironment. *Membranes (Basel)*. 12(2):237.